THE ASTROPHYSICAL JOURNAL, 214:934–945, 1977 June 15

THE OCCULTATION OF EPSILON GEMINORUM BY MARS: ANALYSIS OF McDONALD DATA

TEXAS–ARIZONA OCCULTATION GROUP*

Received 1976 October 8; revised 1976 November 18

ABSTRACT

We present an analysis of observations of the occultation of ϵ Gem by Mars on 1976 April 8. The data were obtained by three neighboring telescopes at McDonald Observatory. Intensity fluctuations on time scales ~ 100 ms were observed simultaneously at the three telescopes. As the observations compare well with predictions of turbulent scintillation theory, we conclude that such fluctuations were probably largely the effect of stellar scintillations in the Martian atmosphere. The stellar diameter is included as a parameter in the theory, but in a way which differs from previously published interpretations of occultations of extended sources by planetary atmospheres. Scintillations govern the experimental uncertainty in the deduction of the scale height of the high Martian atmosphere. We obtain a density scale height of 9.9 ± 2.5 km at an altitude of 74 ± 8 km above the mean surface. For CO_2 gas, this result corresponds to a temperature of 190 ± 50 K.

Subject headings: occultations — planets: atmospheres — planets: Mars — stars: individual

I. INTRODUCTION

On 1976 April 8, Mars occulted ϵ Geminorum in the first major planetary occultation observable from large North American telescopes in over two decades. Although the Martian atmosphere has now become accessible to in situ measurement, results of the ϵ Gem occultation will play an important role in the assessment of the limitations of the stellar occultation technique for application to more remote planetary atmospheres. The principal controversial point which exists at present is the question of the effects of turbulent scintillation on stellar occultation light curves. Young (1976) and Jokipii and Hubbard (1977) present the case for scintillation based upon data up to and including the 1971 Jupiter occultation of β Sco. Elliot and Veverka (1976) use the same data to argue for an alternative model. Consequently, efforts were made to organize observations of the Mars occultation of ϵ Gem so as to provide a better test of the scintillation theory. Ideally, one would wish to have simultaneous observations from telescopes equally spaced along the edge of the shadow zone (projected limb of Mars) with separations ranging from a few hundred meters to several tens of kilometers. For the ϵ Gem events, the correlation distance for scintillations would be expected to be on the order of several kilometers (see below).

The observations reported here were attempted from McDonald Observatory of the University of Texas, with three telescopes separated by no more than about 100 m along the projected Martian limb, and from the Mount Lemmon and Catalina sites of the University of Arizona, with two telescopes separated by 2.5 km along the projected limb. The observations were made in daylight with Mars near the zenith and the Sun near the horizon. The sky over McDonald was clear, and the seeing was good. Unfortunately, moderately dense cirrus cloud cover was present over southern Arizona, and foiled the observations attempted by T. Gehrels and G. Rieke from the University of Arizona telescopes.

The data which we consider here nevertheless make possible a test of the scintillation theory. However, the test is possibly not yet entirely definitive because of the absence of information on the maximum extent of correlation of fluctuations parallel to the limb.

A preliminary deduction of the Martian scale height from data obtained at one of the McDonald telescopes has been published elsewhere (de Vaucouleurs, Nather, and Young 1977). We show here that, as expected, the results from the other telescopes are in good agreement. Scintillation theory indicates that the measurements from the different McDonald telescopes cannot be regarded as independent, and that considerable uncertainty must therefore be assigned to the derived scale height of the mean atmosphere. We proceed to a discussion of the observational material, the theory to be tested, and a comparison of data with theory.

II. OBSERVATIONAL ARRANGEMENTS

Table 1 summarizes the pertinent information for the three McDonald telescopes.

The 36 inch (91 cm) telescope used the de Vaucouleurs photometer with a 1P21 tube, V filter, and Polaroid to reduce sky background and operated in pulse counting mode. The pulses were counted into 10 ms bins which were recorded on cassette tape with clock synchronization. Data control was provided by a 16K memory NOVA computer. The star contributed about 8% of the total signal. A discussion of

* Membership listed at end of paper.

TABLE 1

SUMMARY OF PARAMETERS FOR THE SIX McDONALD OBSERVATIONS

Event	Telescope (inches)	Designation	Observers	Wavelength (Å)	Time Resolution (ms)	Relative Weight
Immersion.....	36	McD 1	de Vaucouleurs, Nather	5500	10	1.0
Emersion.....	36	McD 4	de Vaucouleurs, Nather	5500	10	0.5
Immersion.....	30	McD 2	Africano, Evans	4700	8	0.25
Emersion.....	30	McD 5	Africano, Evans	4700	8	0.5
Immersion.....	107	McD 3	Palm, Silverberg, Wiant	9400	250	1.0
Emersion.....	107	McD 6	Palm, Silverberg, Wiant	9400	250	1.0

the noise level due to terrestrial scintillation and other local effects is given in § IV*c*.

The 30 inch (76 cm) telescope made a single channel recording through the *B* filter, using a sky reducing Polaroid and the blue channel of the two-channel occultation photometer. The data were fed into 8 ms bins on cassette tape controlled by a 16K memory NOVA computer. The star contributed about 4% of the total signal; a discussion of the noise contribution is given also in § IV*c*.

The observations at the 107 inch telescope were made both with a single-channel photometer and an area photometer. The latter was an 11 × 11 silicon diode array, operated at 1".8 per diode in a bandpass from 780 mm to 1100 nm. The integration time was 50 ms, and in this time the sky background on each diode did not reach detector threshold. At the end of each 50 ms frame on the area scan, a 5 ms sample was taken from the single-channel photometer. This instrument had a bandpass of 25 nm centered at 700 nm and recorded transmission through a 20" diaphragm (i.e., star plus planet) and a Polaroid filter. Five frames from the area photometer were coadded in real time and stored in the core of the Varian computer. The five samples from the single-channel photometer were kept at their original time resolution. The 16K storage in the Varian computer permitted 27 s of information to be recorded at the time of disappearance. This was transferred to magnetic tape, and an additional 27 s of data were recorded at reappearance. Preliminary reduction consisted in coadding and plotting those bins in the area array which exceeded threshold which was found to be at about 10% the intensity at the center of the Martian disk.

Neither a "central flash" near the midpoint of the Mars occultation nor a predicted subsequent Phobos occultation was observed at any of the telescopes.

III. SCINTILLATION THEORY—SUMMARY REVIEW

Young (1976) has shown that nominal density fluctuations, comparable to those present in the Earth's atmosphere, can produce significant scintillations in an occultation of a star by a planetary atmosphere. Prior to occultation the star will scintillate because of the turbulence of the Earth's atmosphere. Such terrestrial scintillations depend upon the telescope aperture but have a typical fluctuation time scale ~10 ms for a 60 cm telescope. As the star begins to disappear, terrestrial scintillations decrease proportional to the residual light. The fluctuations which are then observed are predicted to be predominantly produced in the atmosphere of the other planet. For isotropic homogeneous Kolmogorov turbulence with an outer scale much greater than a Fresnel scale, in the Rytov approximation, one may calculate the following quantities (Jokipii and Hubbard 1977):

$$C_p(\alpha) \approx \frac{\int_0^\infty x^{-8/3} dx \sin^2(x^2) J_0(\alpha x)}{\int_0^\infty x^{-8/3} dx \sin^2(x^2)}, \quad (1)$$

where C_p is the autocorrelation function of the scintillations produced by a point source, and α is a dimensionless separation parameter, defined by

$$\alpha = r(4\pi/\lambda D)^{1/2}, \quad (2)$$

where r is the projected separation in the distance planetary atmosphere, λ is the wavelength of the radiation, and D is the distance from the planet to the observer; also we have

$$C_e(\alpha) = \frac{4}{0.770094} \times \int_0^\infty x^{-8/3} dx \sin^2(x^2) J_0(\alpha x) f_1^2(a_{0,\alpha} x), \quad (3)$$

the autocorrelation function for an extended source, normalized such that $C_e(0)$ gives the mean square fluctuation relative to a point source. Here

$$\int_0^\infty x^{-8/3} dx \sin^2(x^2) = \frac{3}{5} \frac{\Gamma(\frac{1}{6}) \cos(5\pi/12)}{2^{1/6}} = 0.770094, \quad (4)$$

$$a_{0,\alpha} = a_0(4\pi/\lambda D)^{1/2}, \quad (5)$$

where a_0 is the projected radius of the occulted star, and the function f_1 is the two-dimensional Fourier transform of the star's brightness distribution. The accuracy of the theory and the data do not justify

inclusion of the small effect of limb darkening; for a uniformly illuminated disk we have

$$f_1(a_{0,\alpha}x) = \int_0^1 ydyJ_0(a_{0,\alpha}xy) = (a_{0,\alpha})^{-1}J_1(a_{0,\alpha}x)\,. \quad (6)$$

Equations (1) and (3) can then be integrated for various values of α to obtain the fluctuation time scales for point and extended sources. To convert α to time, we divide the corresponding separation r (see eq. [2]) by the velocity v with which the star-observer line passes through the Martian atmosphere. In the spirit of the isotropic approximation (discussed by Young), the total velocity, rather than the component parallel to the gravity vector, is used.

In the Rytov approximation, for isotropic Kolmogorov turbulence, the mean-square amplitude of the scintillations, or scintillation power, is given by

$$P_p = LAD^2a^{-7/3} \quad (7)$$

for a point source, where L is the effective path length through the Martian atmosphere, A is a parameter which expresses the amplitude of the turbulent refractivity fluctuations, and

$$a = (\lambda D)^{1/2} \quad (8)$$

is the Fresnel scale. For an extended source, the corresponding scintillation power is

$$P_e = P_pC_e(0)\,. \quad (9)$$

In the case of the occultation by Mars, the diameter of the occulted star is known from a lunar occultation (de Vegt 1976) to be $0''.0056 \pm 0''.0006$, corresponding to a projected radius of 3 km at Mars at the time of the occultation. Equations (3), (7), and (9) thus make specific predictions about the nature of the fluctuations to be observed in the occultation data. There are no free parameters, as the quantity A is already fixed by the observed scintillation parameters for the Earth at fluctuation scales ~ 10 cm, and for Jupiter at scales ~ 0.5 km (Young 1976).

A quick grasp of the predictions can be obtained by referring to Figures 1 and 2. Figure 1 shows the predicted scintillation power, relative to a point source, for a variety of planetary occultations. In addition to parameters for the 1971 occultations of β Sco A and C by Jupiter, and the 1968 occultation by Neptune (discussed by Young), we show parameters for the present Mars occultation and a forthcoming occultation by Uranus in 1977. In the case of ϵ Gem, the stellar diameter is so large that the asymptotic limit $C_e(0) \sim a_{0,\alpha}{}^{-7/3}$ is effectively reached. The wavelength dependence of the scintillation power (see eqs. [7] and [9]) then cancels: the amplitude of the scintillations in the Mars occultations should be essentially independent of wavelength. Figure 1 also indicates that the scintillation power of the ϵ Gem occultation should be substantially less than the β Sco occultations because of the large angular diameter of ϵ Gem. Using equation (9), and making allowance for the differing values of L, the refractivity at the occultation level, and the Fresnel zone size, we find that the scintillation power for ϵ Gem should be approximately 0.0025 of that for the β Sco A occultation. The mean amplitude of the scintillations should then be smaller by a factor ~ 0.05.

Figure 2 predicts the shape of the autocorrelation function for the scintillations. For ϵ Gem, $a_{0,\alpha}$ was approximately 33 at 5000 Å, and 23 at 9400 Å. The square root of $C_e(\alpha)/C_e(0)$ would correspond, in some average sense, to the profile of a typical fluctuation.

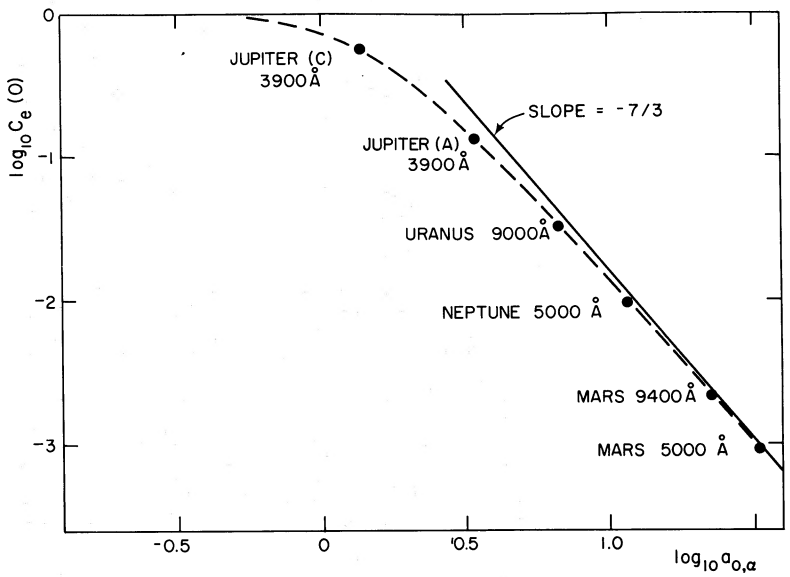

FIG. 1.—Scintillation power of extended sources, relative to a point source, for various planetary occultations

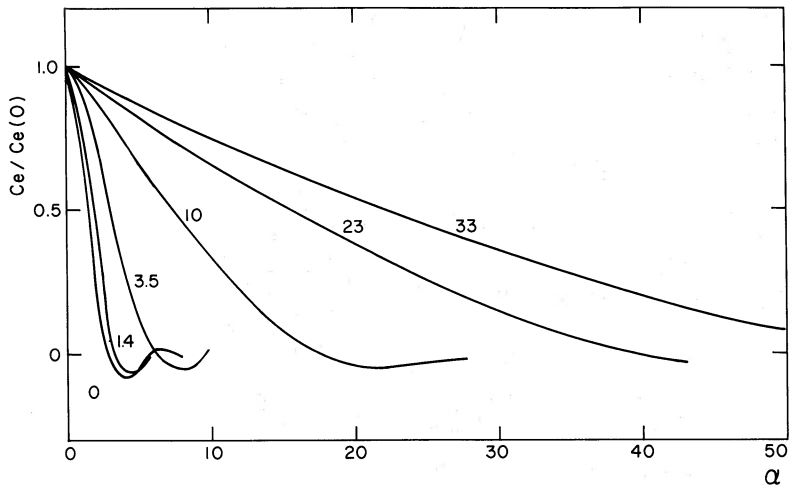

FIG. 2.—Theoretical autocorrelation functions for scintillations of a point source, and for uniform disks of radii $a_{0,\alpha} = 1.4$, 3.5, 10, 23, and 33.

IV. DEDUCTION OF MARTIAN ATMOSPHERIC TEMPERATURE PARAMETERS

a) Data Manipulation

In order to intercompare all six sets of data, the higher time resolution data were initially averaged to the same interval as the 107 inch (248.9 ms), as follows. The centered time of each 107 inch data point was computed, and the nearest data point for the smaller telescopes was then located. The latter were first preaveraged to 100 ms (36 inch) and 96 ms (30 inch) intervals, respectively. To ensure complete coverage, the nearest data point, the data points on either side of it, and 50% of the two next adjacent data points were averaged together to give a data point which could be directly compared with the 107 inch data. Because the effective averaging "window" was approximately 400 ms wide, the data for the smaller telescopes were thus smoothed about 60% more than the data for the 107 inch, which of course used an averaging interval of 250 ms. The effect of the additional averaging is to make the scintillations in the 107 inch data appear slightly stronger than in the other data sets.

The data records were then manipulated to yield the stellar flux as a function of time, $\phi(t)$, normalized such that $\phi = 1$ for the unocculted star. The observed count rate was assumed to be given by the expressions

$$C(t) = S\phi(t) + B_0 + B_1 t\,, \qquad (10)$$

where C is the count rate, S is a constant scale factor, and B_0 and B_1 are constants corresponding to the background signal from Mars and the sky. Prior to occultation, a least-squares fit of a straight line to the data gave $S + B_0$ and B_1; well after occultation, a similar fit gave B_0 and B_1. In the case of the 107 inch data, the constant B_1 was removed by the area scanner at the time of observation, so that only S and B_0 were required to fit the data. It turned out in the case of McD 2, McD 4, and McD 5 that the preoccultation value of B_1 differed significantly from the postoccultation value due to the presence of nonlinear changes in the background level. In the case of McD 2 this was attributable to guiding errors near to, and perhaps during, occultation. For the three light curves where this problem arose, the constants B_0 and B_1 were determined from a long run of data in mid-occultation. The constant S was then determined from a short run of data on the unocculted star just prior to disappearance and subsequent to reappearance.

The constant B_0 is in all six cases based upon mid-occultation data, and is therefore vulnerable to the influence of residual stellar flux. Near mid-occultation at McDonald, the mean ray would have a closest-approach distance ~30 km above the surface of Mars. The residual flux at this level, ϕ_M, depends upon the scale height at this point, and upon the absorbing properties of the atmosphere. Assuming a lossless atmosphere with a scale height of 10 km, and making allowance for the effect of limb curvature, we find $\phi_M \sim 0.013$. We have not attempted to analyze the light curves for $\phi \leqslant 0.10$, so the uncertainty produced by ϕ_M is not large. As ϕ_M is increased from zero to 0.013, the derived scale heights (discussed below) increase by ~5%. This error is small compared with the effects of fluctuations which we attribute to Martian scintillation. In the following, $\phi_M = 0$ is assumed.

The factors affecting the quality of the data, mentioned above, lead to the subjective assignment of relative weights for the six McDonald observations given in Table 1.

Figures 3 and 4 show the light curves for the six observations. The occultations occurred virtually simultaneously at all three telescopes; the light curves are all plotted with no relative shift in the time argument for McD 5, where a delay of approximately 4 s in mid-occultation, probably incurred during tape-changing, necessitated a corresponding correction to the time.

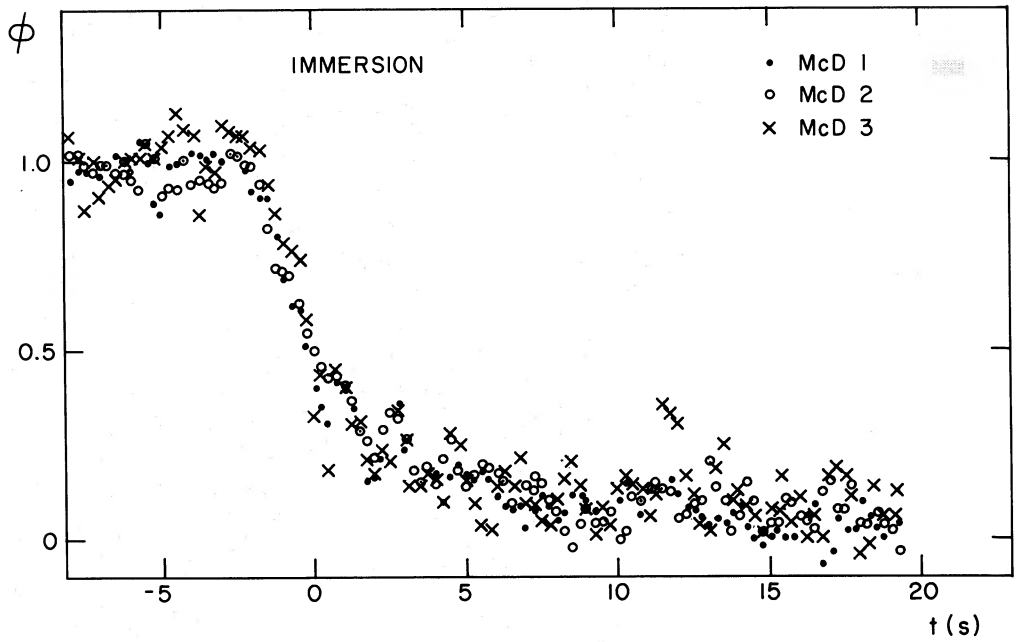

FIG. 3.—Immersion light curves for the three McDonald telescopes, at 250 ms time interval. In this and in all figures showing immersion data, time increases to the right.

b) Timing and Astrometric Data

Circumstances of the occultation at McDonald are shown in Figure 5. The shadow velocity was 21.69 km s^{-1} eastward and 2.17 km s^{-1} southward. The velocity component normal to the limb was 20.02 km s^{-1}, and 8.63 km s^{-1} parallel to the limb. All three telescopes could be enclosed within a circle of ~60 m radius, whereas the Fresnel scale (at 5000 Å) and projected stellar radius were 330 m and 3000 m, respectively. Thus the fluctuations in the occultation light curve would be expected to be well correlated among the three data sets, with the dominant fluctuation time scale of the order of 3 km/22 km s^{-1}

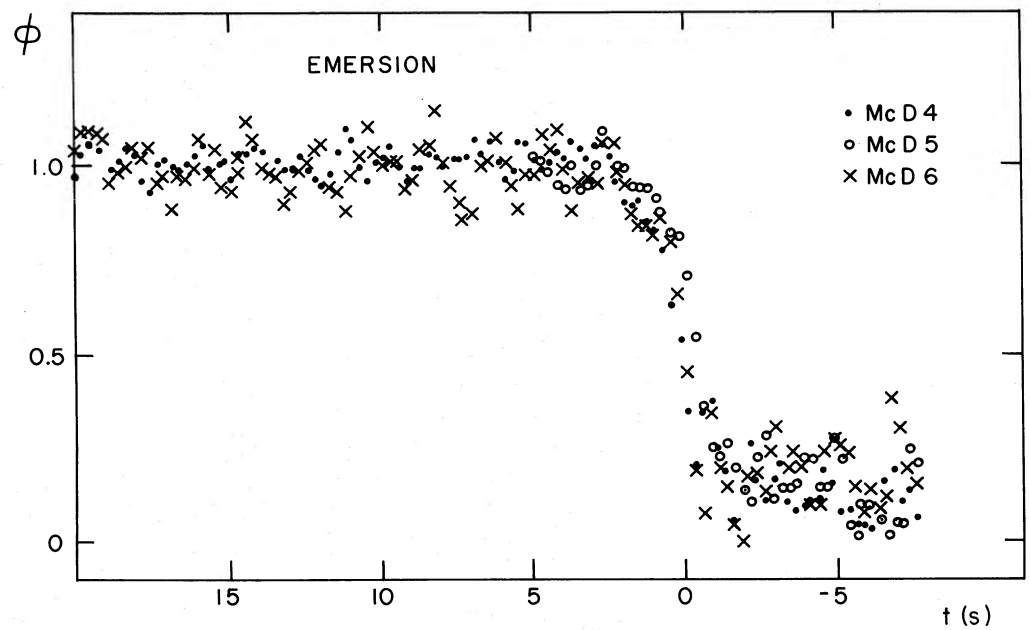

FIG. 4.—Emersion light curves for the three McDonald telescopes, at 250 ms time interval. Time increases to the left in all figures showing emersion data.

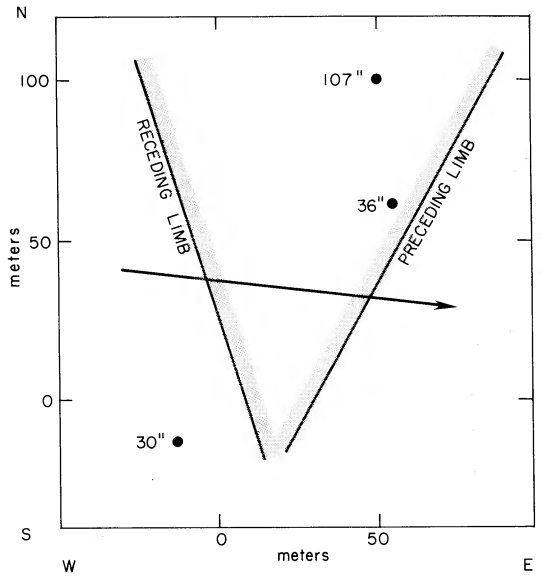

FIG. 5.—View from Mars of the three McDonald telescopes and relative orientation of the shadow. Arrow shows the relative velocity vector.

~140 ms. The relative time separation for occultation at the three telescopes would not exceed 5 ms and was thus undetectable.

The effect of dispersion in the Martian atmosphere would produce a small shift in fluctuation arrival times at the three telescopes. Assuming pure CO_2 gas, the refractivity at a given pressure varies by ~2%–3% from 4700 Å to 9400 Å. At a light level $\phi \approx 0.2$, a given scintillation at 4700 Å would be shifted by ~0.4 km relative to the scintillation at 5500 Å, corresponding to a time shift ~20 ms. The shift would not be readily detectable in the presence of high-frequency noise, although it may be apparent when the data have been further analyzed.

The occultation times reported here have been referred, as is customary, to the estimated times of half-intensity, i.e., $\phi = \frac{1}{2}$. All six light curves were fitted, by least-squares, with the usual theoretical curve for an atmosphere with constant scale height:

$$(\phi^{-1} - 2) + \ln(\phi^{-1} - 1) = v_p(t - t_0)/H, \quad (11)$$

where v_p is the perpendicular velocity component of 20 km s^{-1}, t_0 is the time of half-intensity, and H is the scale height. It was found that t_0 was not strongly correlated with H, and varied by ~ ± 100 ms depending on the data interval which was used for the least-squares fit. As noted above, half-intensity times for the McD 1 and McD 3, and McD 4 and McD 6, respectively, were in good agreement. The deduced half-intensity times are:

$$t_0, \text{ immersion} = 0^h55^m30^s.8 \pm 0^s.1 \text{ UTC}, \quad (12)$$

$$t_0, \text{ emersion} = 1^h00^m22^s.5 \pm 0^s.1 \text{ UTC}, \quad (13)$$

where the errors are estimated rather than formal.

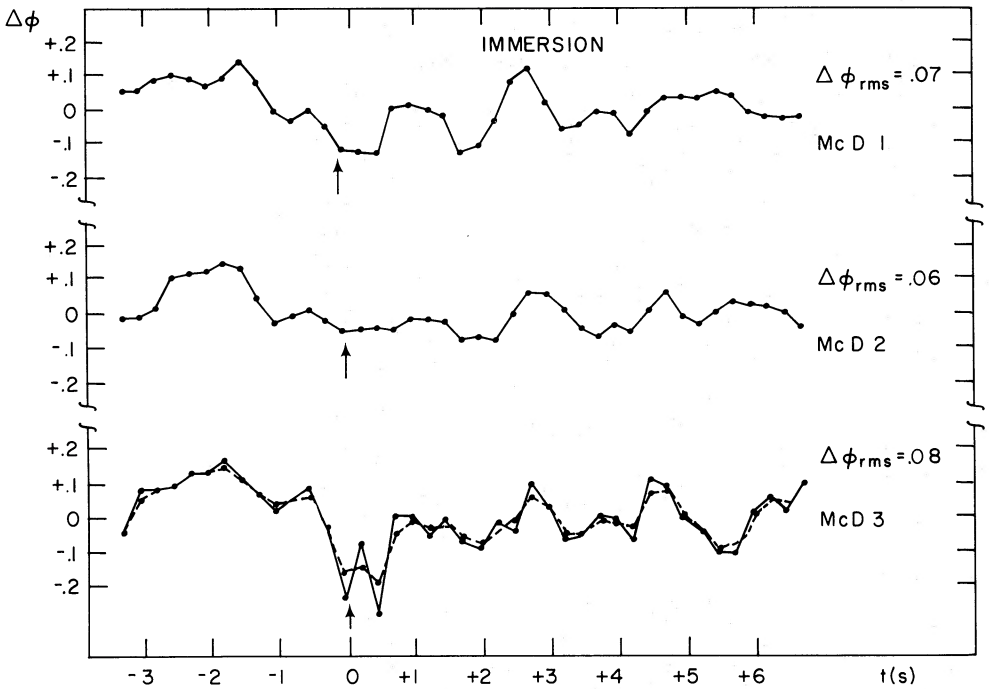

FIG. 6.—Scintillations observed during immersion. Dashed curve shows the effect of smoothing the 107 inch data to the same time resolution (~400 ms) as the other two curves. The rms fluctuation is calculated for the 400 ms data. Arrows show the times of the half-intensity from least-squares fitting of eq. (11).

The timings are in good agreement with an independent determination for McD 1 and McD 4 alone (de Vaucouleurs, Nather, and Young 1977).

The above timings, as well as those from other stations, have been analyzed by Taylor (1977). Taylor finds that the half-intensity points define a surface with oblateness 0.0136, while the solid surface of Mars can be represented by an oblate spheroid with oblateness 0.0057 (Jordan and Lorell 1975). This discrepancy, although possibly real, will be treated here as an indication of the uncertainty in the determination of the half-intensity level in the atmosphere. The equatorial radius of Taylor's half-intensity spheroid is 3465 km + H, while the mean equatorial radius of the solid surface is 3393 km (Jordan and Lorell 1975). We adopt $G = 10$ km, and use a gravity $g = 357$ cm s^{-2} at the half-intensity level.

Using Taylor's solution, we find that immersion occurred on the Martian night hemisphere, at 0400 local solar time, at 49°.4 S latitude and about 330° longitude. At half-intensity, the point of closest approach of the mean ray from the star to the observers was 66 km above the mean surface. Emersion occurred at 1600 local solar time, at 4°.0 N latitude and 150° longitude. The point of closest approach was 82 km above the mean surface.

For immersion and emersion, then, we assume the point of closest approach at half-intensity to correspond to an altitude above the solid surface of 74 ± 8 km.

c) *Analysis of Fluctuations*

In this section we will use the occultation data to test the hypothesis that the statistics of the fluctuations in the light curves can be described by the theory outlined in § III. The results will then form the basis for an analysis of the errors in the scale height determination, which is to be presented in a following section.

Because the average light from the star is changing during occultation, it is not simple to form meaningful residuals for the purpose of analyzing fluctuations. A strictly quantitative comparison of the data with the theory can therefore not be made. However, the following procedure turns out to be useful for a qualitative comparison. For each data point in a light curve, we calculate a running mean of the $2N + 1$ data points which are centered on the given data point. The current value of ϕ is then subtracted from the running mean to yield a residual. After the array of residuals has been formed, the residuals are then corrected to zero mean by subtracting a constant. The obvious alternative procedure, where one fits a model light curve to the data and then calculates the resulting point-by-point residuals, perhaps multiplying by the model value of ϕ^{-1}, does not seem clearly preferable in view of the crudity of the theory and limited number of data points.

Figures 6 and 7 show the resulting residuals at 250 ms intervals (400 ms effective time resolution), over a 10 s interval which extends roughly from $\phi \sim 0.99$ to $\phi \sim 0.10$. At this time resolution, the typical fluctuation is of the order of 1 s in duration. Clearly the value of N in the averaging procedure must be large enough to include several such fluctuations in order to obtain meaningful results. In practice we found that $N = 8$ (corresponding to $2N + 1 \approx 4$ s) gave reasonable results. Unfortunately, such

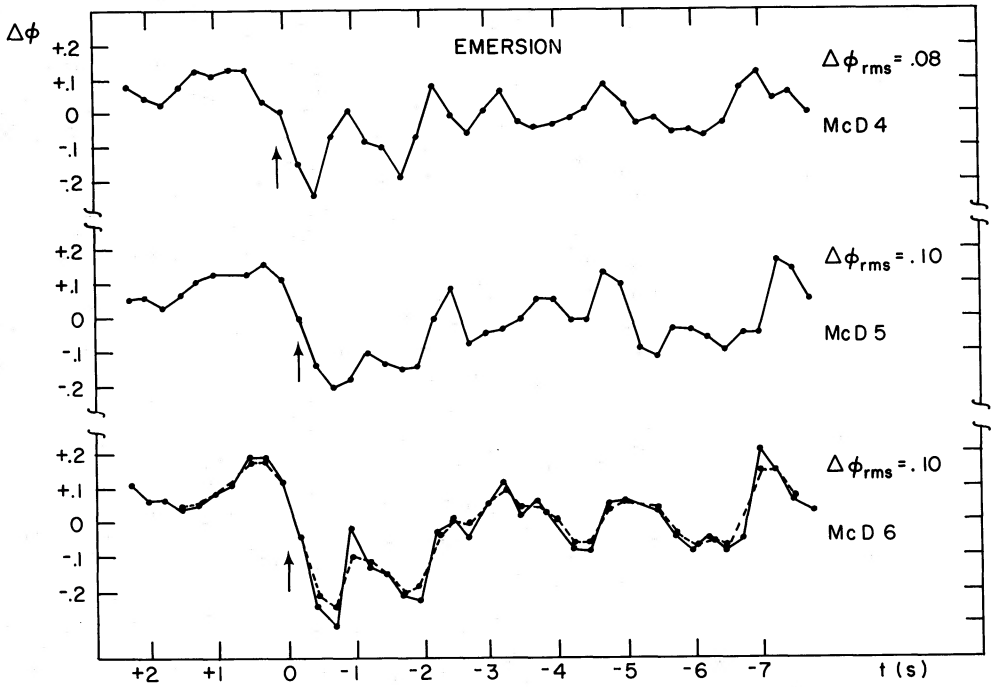

FIG. 7.—Same as Fig. 6, but for emersion

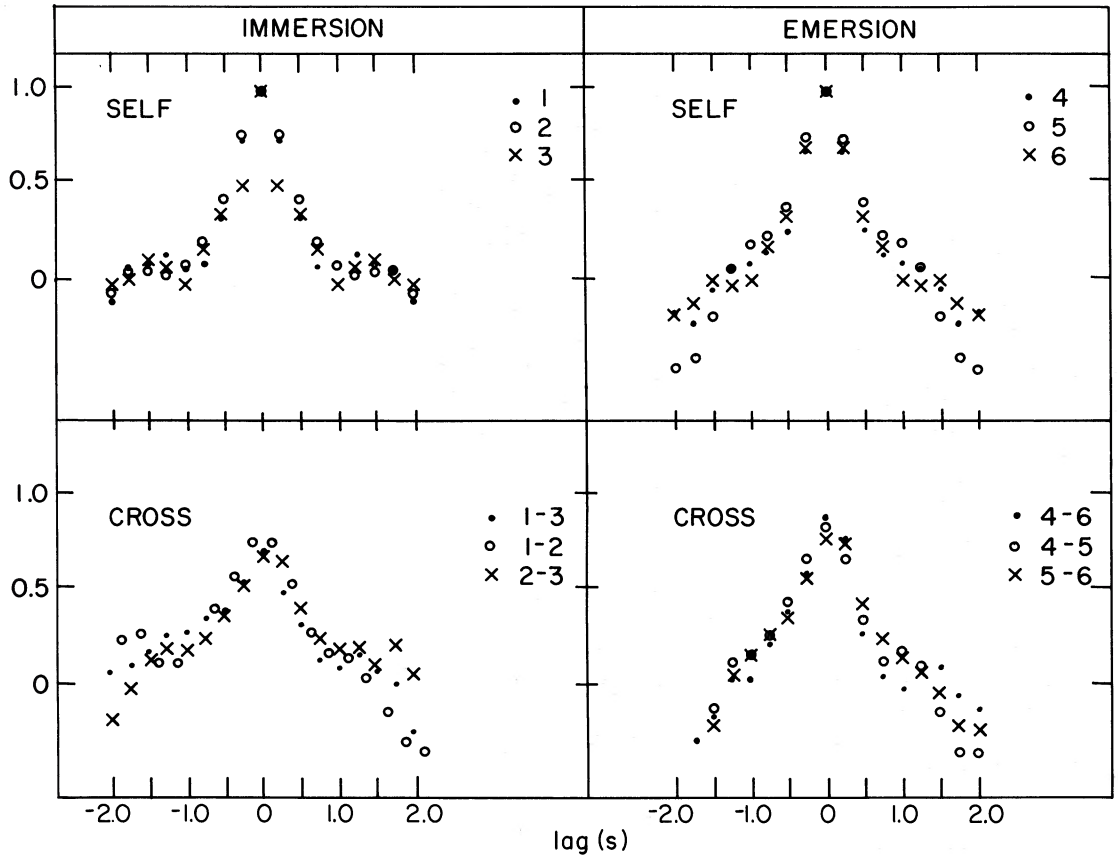

FIG. 8.—Self- and cross-correlation functions for the scintillations shown in Figs. 6 and 7

a large averaging interval fails to filter out systematic changes in the light level in the vicinity of the half-intensity point.

Note that (*a*) there is evident correlation in the fluctuations for the three telescopes in Figures 6 and 7, respectively; (*b*) the rms fluctuation does not change significantly with wavelength.

The fluctuations in Figures 6 and 7 have been cross-correlated and self-correlated in order to demonstrate that good correlation in fact exists among the three telescopes. Figure 8 shows the results of the analysis. The close resemblance of the correlation functions for immersion and emersion, respectively, verifies that essentially the same fluctuations were observed during occultation by the three telescopes. This proves that these fluctuations are largely produced by the Martian atmosphere since terrestrial scintillations are entirely uncorrelated over separations of tens of meters.

Figure 8 cannot be used for comparison with theory as the fluctuations are not resolved. In order to use the 10 ms and 8 ms data for this purpose, it is necessary to carefully evaluate the effects of terrestrial scintillation. Figure 9 shows the self-correlation of residuals in the 36 inch data at 10 ms resolution. The residuals were formed in the same manner as at lower time resolution: a running average over 4 s was subtracted from the current value, and the residuals were then corrected to zero mean. In each case, the correlation function was normalized to unity at zero

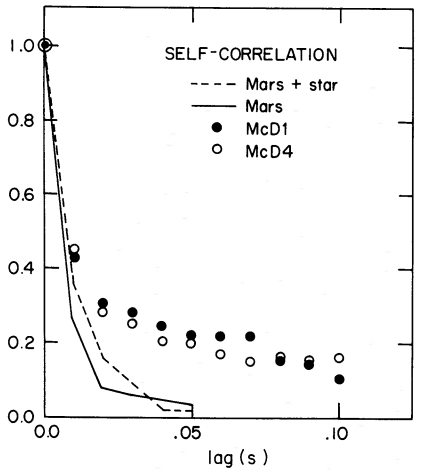

FIG. 9.—Self-correlation of residuals during immersion and emersion for 36 inch telescope. The self-correlation for the terrestrial component is shown with dashed line (Mars plus unocculted star) and solid line (Mars alone).

lag. Figure 9 verifies that, in telescopes of this aperture, the disk of Mars scintillates much like a star, with a correlation time ~10 ms (Young 1969). The self corrections during occultation were formed using a 10 s run of data commencing (or terminating) at $\phi = 0.95$ as determined from the least-squares fit. During occultation, the self correlation is a composite of terrestrial and Martian scintillation. The two may be separated by using the data for the *terrestrial* scintillation of Mars alone, and by assuming that terrestrial scintillation of the star is negligible during occultation. In this case, a scintillation during occultation, in units of the unocculted stellar intensity, is given by

$$\Delta\phi = (\Delta\phi)_t + (\Delta\phi)_m , \qquad (14)$$

where t and m denote the terrestrial and Martian components of the scintillation, respectively. Then

$$\langle(\Delta\phi)^2\rangle = \langle(\Delta\phi)_t{}^2\rangle + \langle(\Delta\phi)_m{}^2\rangle . \qquad (15)$$

and $\langle(\Delta\phi)_t{}^2\rangle$ is separately measurable from the data run with the star absent. At 10 ms time resolution, we obtain the results listed in Table 2.

Table 2 shows that Martian scintillations were observed at essentially the same power level in all four events, and the deduced power level is consistent with that obtained from the time-averaged data, where terrestrial scintillations are suppressed. However, Martian scintillations comprise ~30% of the scintillation power in the 36 inch data, but only ~15% of the scintillation power in the 30 inch data. Thus deduction of the autocorrelation function for the Martian scintillations in the 30 inch data is at best a marginal enterprise. The spurious correlations introduced by the finite length of the time series and by incomplete filtering of the average occultation are at the level of 5%–10%. The error multiplication factor for the 30 inch data is $(0.15)^{-1} = 6.7$, and for the 36 inch data, $(0.3)^{-1} = 3$. Thus the Martian scintillation autocorrelation function can be recovered with a useful degree of accuracy only for McD 1 and McD 4. Of course, an alternative procedure for extracting this function is to cross-correlate McD 1–McD 2, and McD 4–McD 5, thereby suppressing the terrestrial component which would be uncorrelated between the two telescopes. The maximum correlation between the two data sets, at 10 ms, would be expected to be $\sim(0.15 \times 0.3)^{1/2} = 0.21$. In fact, a correlation peak 70% of the expected value occurs at zero lag in both cases, but the correlation function lies too close to the noise level to be of use in testing the theory.

TABLE 2

SCINTILLATION AND NOISE CHARACTERISTICS FOR THE 30 INCH AND 36 INCH OBSERVATIONS*

Event	$\langle(\Delta\phi)^2\rangle^{1/2}$	$\langle(\Delta\phi)^2\rangle_m/\langle(\Delta\phi)^2\rangle$	$\langle(\Delta\phi^2)\rangle^{1/2}{}_m$
McD 1...	0.18	0.27	0.09
McD 2...	0.21	0.15	0.08
McD 4...	0.18	0.33	0.10
McD 5...	0.21	0.15	0.08

* At 10 ms time resolution, for 100 data point intervals.

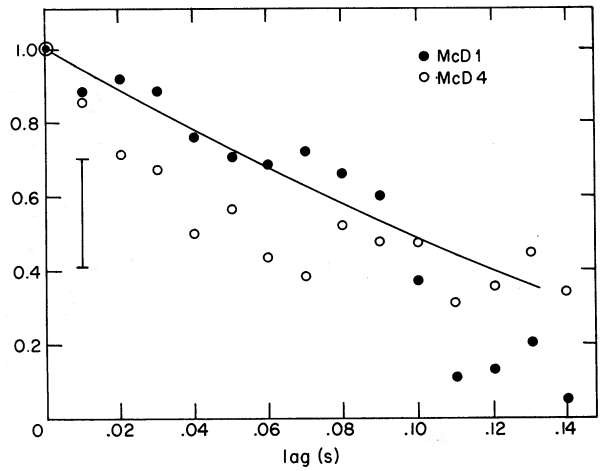

FIG. 10.—Self-correlation of residuals for McD 1 and McD 4, after removal of the terrestrial scintillation. Error bar shows the estimated uncertainty in subtraction of the terrestrial background. Solid curve is from the theory (Fig. 2), assuming a projected stellar disk of 3 km radius.

Figure 10 shows the corrected autocorrelation function for Martian scintillations alone in McD 1, McD 4, compared with a theoretical curve for the assumed radius of ϵ Gem. Data for McD 2 and McD 5 are also consistent with the theory, but the comparison is not meaningful because of the high noise level at 10 ms time resolution. At 400 ms, where terrestrial scintillation is suppressed, Figure 8 shows that the correlation functions for the two telescopes have similar width.

We conclude that a compelling case has been made for the hypothesis that the detailed fluctuations in occultation light curves are produced by scintillations in the occulting planet's atmosphere. The character of the scintillations agrees in essentially all respects with the predictions of § II. We may observe at this point that the maximum intensity excursions in the β Sco A occultations were of the order $\Delta\phi \sim 1.0$ (Elliot and Veverka 1976). Thus, from § II, we would expect the maximum fluctuations in the ϵ Gem data to be of the order $\Delta\phi \sim 0.05$. The observed fluctuations are within a factor of ~2 of this expected value.

Figures 6 and 7 reveal no evident trend in the duration of the fluctuations during occultation. The velocity of the average ray perpendicular to the limb declines from 20 km s^{-1} at $\phi = 0.99$ to 2 km s^{-1} at $\phi = 0.10$, while the velocity parallel to the limb remains constant at 8.6 km s^{-1}. The fact that there is no evidence in the data for a twofold increase in the time scale indicates that a compensating effect, perhaps related to compression of the perpendicular scale as suggested by Young (1976), is in fact operating. In any case, the data appear to be consistent with isotropic turbulence theory.

d) Scale Height Determination

The scale height of the Martian atmosphere was determined by carrying out a least-squares fit of equation (11) to the six occultation light curves. The significant data interval for performing the fit was established by the results of the fluctuation analysis of the preceding section. It was found that the peak cross correlation decreased significantly as more than 40 time-averaged data points (10 s of data) were included. Thus the fitting interval was taken to be the 10 s interval from $\phi \sim 0.99$ to $\phi \sim 0.10$.

The closeness of fit of the data to an isothermal atmosphere curve was investigated by performing a partial inversion of the data using standard techniques (Hubbard *et al.* 1972). The depth of penetration of the average ray into the Martian atmosphere is given by

$$h = v_p \int_{t_0}^{t} dt' \phi(t') , \qquad (16)$$

where t_0 is an arbitrary starting time where $\phi \approx 1$. The bending angle θ is then given by

$$D\theta = v_p \int_{t_0}^{t} dt' [1 - \phi(t')] . \qquad (17)$$

For an isothermal atmosphere, $\ln (D\theta) \propto h/H$. Figures 11 and 12 show the results of an application of equations (16) and (17) to the data; the straight lines correspond to constant scale heights deduced by direct least-squares fitting of equation (11) to the data. One could then proceed further to perform an Abel inversion on the deduced $\theta(h)$ relation to obtain the refractivity profile, $\nu(h)$. This additional step is unwarranted if excursions in the light curve are caused not by radially layered temperature variations, but by random phase changes produced by turbulence in the Martian atmosphere. In this case the information content of the light curve is sufficient only to extract a single scale height measurement together with t_0. Further discussion of this matter follows.

As the McDonald telescopes were all observing effectively the same scintillations produced in Mars's atmosphere, the discrepancies between telescopes in the scale heights deduced for a single event, either immersion or emersion, is an indication of the error introduced by local factors such as terrestrial scintillation, background noise, and guiding errors. On the other hand, the much larger difference between the average immersion and average emersion scale height must be related to the scintillation in Mars's atmosphere. It is not likely that the scale height difference is real, since this hypothesis would require that the predawn Martian atmosphere be ~ 60 K warmer than the midafternoon atmosphere. We will now show that such a large error is easily understood in terms of the character of the scintillations.

It is well established that the deduction of a scale height from an occultation record is sensitive to a systematic error in the stellar intensity, ϕ. The sensitivity depends to some degree on the portion of the light curve where the fit is carried out, but typically an error of ~ 0.10 in ϕ produces $\sim 100\%$ error in H (Hubbard *et al.* 1972). Thus, if we have on the order of one data point for ϕ which is in error by $\sim 10\%$, the resulting error in H resulting from fitting that data point is $\sim 100\%$. Now if we have n data points normally distributed about the "true" curve with a

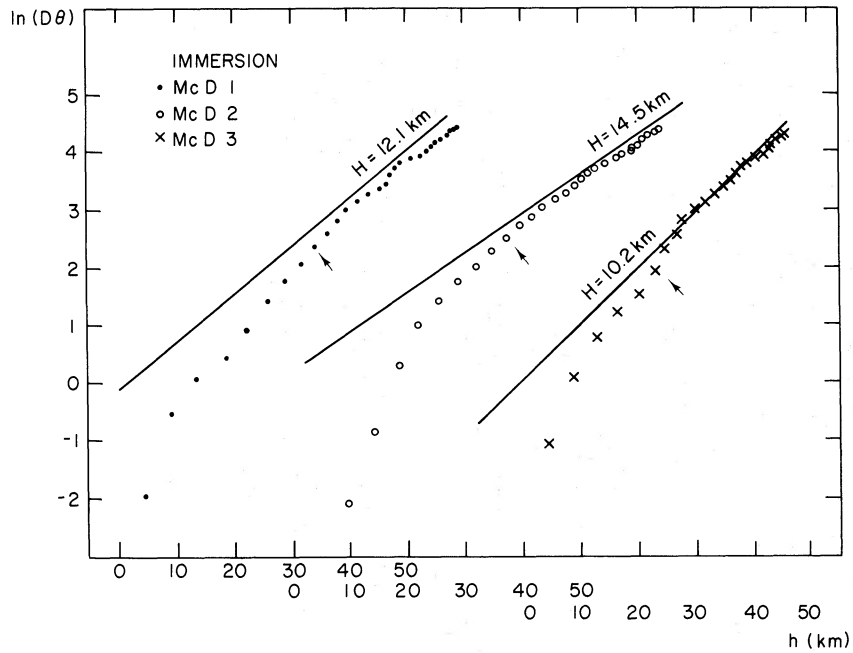

FIG. 11.—Bending angle versus depth relations for immersion data. Arrows show half-intensity points.

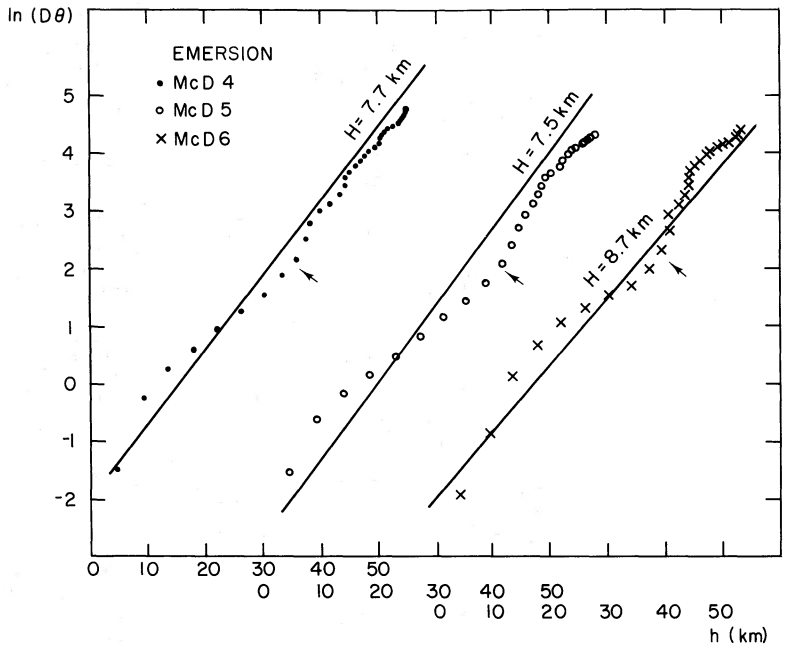

FIG. 12.—Same as for Fig. 11, but for emersion

dispersion $\Delta\phi$, we may write for the error ΔH:

$$\Delta H/H \approx 10\Delta\phi/\sqrt{n}\,. \qquad (18)$$

Although 40 data points were used for each scale height determination, the number of independent measurements is much smaller because the fluctuations tend to be correlated. From Figures 6 and 7, we estimate $n \approx 10$ for the 250 ms data. Since $\Delta\phi \approx 0.08$, the predicted error in H is $\sim 25\%$. Under these circumstances, there is no point in attempting to deduce variations in H from the data. We may mention that a more elaborate χ^2 analysis of the data gives essentially the same result.

Since ϵ Gem's large diameter tended to suppress scintillations, it may at first seem surprising that scintillations produce such large errors. The basic problem is that ϵ Gem's diameter was about 60% of the scale height, and since the light curve could not be followed past $\phi \approx 0.10$ because of the large background, not very many independent scintillations are contained in the light curve.[1]

The large stellar diameter also biases the light curve toward a spuriously large scale height, but this effect can be shown to be no more than a few percent and thus negligible compared with other error sources.

The weighted average of our six scale-height measurements is then $H = 9.9 \pm 2.5$ km. For CO_2 gas, this corresponds to a temperature of 190 ± 50 K. At the half-intensity point, the refractivity is then $9.5 \pm 3.5 \times 10^{-10}$, the pressure 1.5 ± 0.8 μbars, and the number density $5.6 \pm 2.0 \times 10^{13}$ cm^{-3}. These results are shown on Figure 13, along with a model atmosphere calculated by McElroy (1969) and Viking data from Nier *et al.* (1976).

[1] For comparison, the β Sco A data for Jupiter (Hubbard *et al.* 1972) contained approximately 60 independent measurements with $\Delta\phi \equiv 0.10$ at a time resolution ~ 2 s. Thus $\Delta H/H \sim 0.1$, in agreement with the χ^2 test.

V. CONCLUSIONS

The results of the above analysis are in general agreement with theoretical predictions about scintillation in stellar occultation light curves (Young 1976;

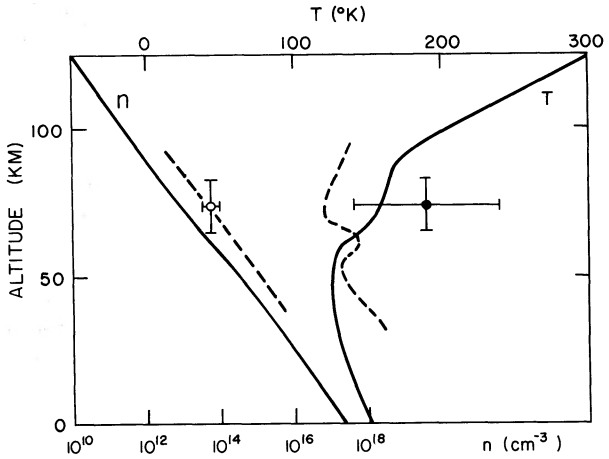

FIG. 13.—Comparison of occultation measurement of density (*open circle*) and temperature (*closed circle*) with McElroy (1969) model atmosphere. Dashed curves are *Viking* entry measurements (Nier *et al.* 1976). Pure CO_2 is assumed.

Jokipii and Hubbard 1976). The relatively large stellar diameter limits the number of independent scintillations observed in the light curve. Thus considerable uncertainty is introduced into the scale height determination, even though scintillations cause no significant systematic bias (Hubbard and Jokipii 1977).

The amplitude of the fluctuations in the ϵ Gem data is in reasonable agreement with that predicted from scintillation theory by scaling from observed fluctuations in the Jupiter–β Sco occultations. Thus we conclude that the degree of turbulence in the Martian and Jovian atmosphere is similar. Although there is some indication of slightly greater turbulence in the daytime atmosphere of Mars as compared with the nighttime, the difference may not be significant.

Our analysis demonstrates a possible procedure deducing stellar diameters from a statistical analysis of occultation intensity fluctuations. It is clear from the results that this procedure is not particularly to be recommended as a high-precision technique. Thus, on the basis of a turbulence model, we reach somewhat different conclusions than those of Elliot, Rages, and Veverka (1976). For further discussion of this point, the reader should consult Jokipii and Hubbard (1977). The reader should likewise refer to Elliot *et al.* (1977) for alternative interpretations of Mars–ϵ Gem data.

Although we believe that we have constructed a strong circumstantial case for turbulent scintillation in stellar occultations by planetary atmospheres, the case must still be regarded as basically unproved. Still lacking are definitive data on the extent of correlations parallel to the limb. Nevertheless, the turbulence model makes it possible to assign conservative, and we think realistic, error bars to occultation measurements of scale heights. For the present, then, it would seem prudent for this model to be considered as a likely explanation for the fine scale fluctuations in the light curve.

Finally, we should observe that the particular circumstances of a given stellar occultation will determine the degree of accuracy which can be realized from a single scale height measurement. Terrestrial planet occultations tend to be more disadvantageous because of the relatively small ratio of scale height to Fresnel scale or projected stellar diameter. Thus the generous error bars attached to our results here are not necessarily indicative of those for a giant-planet occultation such as Jupiter–β Sco. The best way to overcome the effects of scintillation, if they are as pronounced as we claim, is to suitably average a number of independent, high quality observations of the same event.

We thank J. L. Elliot, D. M. Hunten, and A. T. Young for comments on versions of this paper and B. Wilking for assistance in the correlation analysis. This work was supported in part by the following grants: NSF-AST 74-23135 (D. S. E.), NASA NSG-7045 (W. B. H.), and NASA NSG-7101 (J. R. J.).

REFERENCES

de Vaucouleurs, G., Nather, R. E., and Young, P. J. 1977, *A.J.*, **81**, 1147.
de Vegt, C. 1976, *Astr. Ap.*, **47**, 457.
Elliot, J. L., Rages, K., and Veverka, J. 1976, *Ap. J.*, **207**, 994.
Elliot, J. L., French, R. G., Dunham, E., Gierasch, P. J., Veverka, J., Church, C., and Sagan, C. 1977, *Science*, **195**, 485.
Elliot, J. L., and Veverka, J. 1976, *Icarus*, **27**, 359.
Hubbard, W. B., and Jokipii, J. R. 1977, *Icarus*, **30**, 531.
Hubbard, W. B., Nather, R. E., Evans, D. S., Tull, R. G., Wells, D. C., van Citters, G. W., Warner, B., and Vanden Bout, P. 1972, *A.J.*, **77**, 41.
Jokipii, J. R., and Hubbard, W. B. 1977, *Icarus*, **30**, 537.
Jordan, J. F., and Lorell, J. 1975, *Icarus*, **25**, 146.
McElroy, M. B. 1969, *J. Geophys. Res.*, **74**, 29.
Nier, A. O., Hanson, W. B., Seiff, A., McElroy, M. B., Spencer, N. W., Duckett, R. J., Knight, T. C. D., and Cook, W. S. 1976, *Science*, **193**, 786.
Taylor, G. E. 1977, *Nature*, in press.
Young, A. T. 1969, *Appl. Optics*, **8**, 869.
———. 1976, *Icarus*, **27**, 335.

J. Africano, G. de Vaucouleurs, D. S. Evans, B. E. Finkel, R. E. Nather, C. Palm, E. Silverberg, and J. Wiant: Department of Astronomy, University of Texas, Austin, TX 78712

W. B. Hubbard: Department of Planetary Sciences, Lunar and Planetary Laboratory, University of Arizona, Tucson, AZ 85721

J. R. Jokipii: Department of Planetary Sciences, Department of Astronomy, University of Arizona, Tucson, AZ 85721